Spin transition rates in nanowire superlattices: Rashba spin–orbit coupling effects

Sanjay Prabhakar[1]**, Roderick Melnik**[1,2] **and Luis L Bonilla**[2,3]

[1] M²NeT Laboratory, Wilfrid Laurier University, Waterloo, ON, N2L 3C5, Canada
[2] Gregorio Millan Institute, Universidad Carlos III de Madrid, 28911, Leganes, Spain
[3] School of Engineering and Applied Sciences, Harvard University, Cambridge, MA 02138, USA

Abstract
We investigate the influence of Rashba spin–orbit coupling in a parabolic nanowire modulated by longitudinal periodic potential. The modulation potential can be obtained from realistically grown superlattices (SLs). Our study shows that the Rashba spin–orbit interaction induces the level crossing point in the parabolic nanowire SLs. We estimate large anticrossing width (approximately 117 μeV) between singlet–triplet states. We study the phonon and electromagnetic field mediated spin transition rates in the parabolic nanowire SLs. We report that the phonon mediated spin transition rate is several order of magnitude larger than the electromagnetic field mediated spin transition rate. Based on the Feynman disentangling technique, we find the exact spin transition probability. For the case wave vector $k = 0$, we report that the transition probability can be tuned in the form of resonance at fixed time interval. For the general case ($k \neq 0$), we solve the Riccati equation and find that the arbitrary values of k induces the damping in the transition probability. At large value of Rashba spin–orbit coupling coefficients for ($k \neq 0$), spin transition probability freezes.

(Some figures may appear in colour only in the online journal)

1. Introduction

Low-dimensional semiconductor nanostructures such as quantum dots, quantum wells and quantum wires can be formed in the plane of two-dimensional electron gas (2DEG) with the application of externally applied gate potentials, have attracted significant interest for building robust spintronics logic devices and other applications [1–9]. Single electron spins in these nanostructures can be manipulated by several parameters such as the gate controlled electric fields in the lateral direction and externally applied magnetic fields. The Rashba and Dresselhaus spin–orbit couplings provide another efficient way to control the single electron spins in these nanostructures [1, 6, 10]. The Rashba spin–orbit coupling arises due to structural inversion asymmetry in the crystal lattice along the growth direction [11]. The Dresselhaus spin–orbit coupling arises due to bulk inversion asymmetry in the system [12].

Accurate estimation of the spin transition rate, mediated by phonons and electromagnetic fields, is of great interest for the design of optoelectronic devices [7, 13, 14]. Long spin relaxation rates, approximately 0.85 ms in GaAs quantum dots and 20 ms in InGaAs quantum dots, have been measured by utilizing several different experimental techniques such as pulsed relaxation and optical orientation methods [15, 16]. In these experiments, it is confirmed that the transition rate is dominated by the spin–orbit coupling with respect to the environment [2, 17, 18]. Because of the spin–orbit coupling, the electron spin qubits in the nanowire quantum dots localized in a transmission line resonator can be manipulated, stored and read out with the application of the gate controlled electric fields [13, 19]. In this paper, we investigate the energy spectrum of the parabolic nanowire modulated by realistically grown superlattices (SLs) in the longitudinal direction [20–22]. We focus on the study of the crossing of the energy spectrum of the nanowire SLs accounting for the Rashba spin–orbit coupling. The crossing point can be achieved with the accessible values of the strength of the Rashba spin–orbit coupling. We investigate the spin transition rate in parabolic nanowire SLs
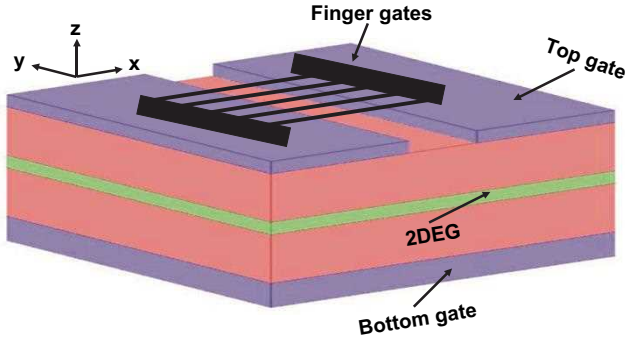
Figure 1. Schematic diagram of the proposed experimental setup of the parabolic NWSLs periodically modulated by an external potentials via finger gates. The 2DEG can be realized in InAs quantum well by sandwitching between two GaAs barrier materials. The top gate induces the parabolic NWSLs while the bottom gate control the strength of the Rashba spin–orbit coupling.

with the Rashba spin–orbit coupling under the influence of electromagnetic field radiation [23, 24], phonons [18] and Dyakonov–Perel (DP) [25] mechanisms. We can write the momentum as a classical variable in the DP mechanism under the Markovian process [25–27] and estimate the transition probability by utilizing the Feynman disentangling technique method [2, 28, 29]. The DP mechanism corresponds to the spin splitting of the conduction band in zinc blende semiconductors at finite wave vectors which is equivalent to the presence of an effective magnetic field that causes the precession of an electron spin [25, 26].

The paper is organized as follows: in section 2, we develop a theoretical model that allows us to find the crossing of the energy spectrum of the parabolic nanowire SLs with the Rashba spin–orbit coupling. In this section, we also develop the theoretical model that allows us to find the spin transition rate. In section 3, we plot the dispersion relation (see figure 1) of the parabolic nanowire modulated by longitudinal periodic potential. In figures 2 and 3, we plot the spin transition rate of the nanowire SLs with the Rashba spin–orbit coupling via electromagnetic field radiation, phonons and DP mechanisms. Finally, in section 4, we summarize our results.

2. Theoretical model

The total Hamiltonian of the quasi-one-dimensional parabolic nanowire formed in the plane of 2DEG with the Rashba spin–orbit coupling in the presence of longitudinal modulation potential (see figure 1 for experimental set up) can be written as [4, 30–33]

$$H = H_{xy} + H_z + H_R, \qquad (1)$$

$$H_{xy} = \frac{p_y^2}{2m} + \frac{1}{2}m\omega_0^2 y^2 + \varepsilon_\nu(k), \qquad (2)$$

$$H_z = p_z^2/2m + V(z), \qquad (3)$$

$$H_R = \frac{\alpha}{\hbar}\left(p_y\sigma_x - p_x\sigma_y\right), \qquad (4)$$

where H_z is the Hamiltonian of the electrons along the z-direction and H_R is the spin–orbit Hamiltonian associated

with the Rashba coupling. The full descriptions of H_z and H_R will be discussed shortly. In the above Hamiltonians p_x, p_y and p_z are the momentum operator, m is the effective mass, α is the strength of the Rashba spin–orbit coupling and $\omega_0 = \hbar/m\ell_0^2$ is the confinement frequency of the parabolic potential with ℓ_0 being the oscillator strength. σ_i ($i = x, y, z$) are the Pauli spin matrices. $\varepsilon_\nu(k)$ provides the periodic longitudinal modulation potential along the x direction in the form of: [4, 34, 35]

$$\varepsilon_\nu(k) = \frac{\Delta_1}{2}\left(1 - \cos kl\right), \qquad (5)$$

where Δ_1 is the first miniband width and l is the SL period [21, 36]. The second term in (1) represents the Hamiltonian of the electron along the z-direction where V_z is the asymmetric triangular quantum well confining potential along the z-direction. Usually, the asymmetric triangular quantum well potential can be found by solving the Schrödinger–Poisson equations self-consistently [1, 37]. The potential along the z-direction can be chosen as $V_z = eEz$ for $z \geqslant 0$ and $V_z = \infty$ for $z < 0$ [38]. The ground state wavefunction ($\Psi_{0z}(z)$) of H_z can be written in the form of Airy function (Ai) as [1, 37, 38]

$$\Psi_{0z}(z) = 1.4261q^{1/2}\text{Ai}\left(qz + \varphi_1\right), \qquad (6)$$

where $\varphi_1 = -2.3381$ is the first zero of the Airy function and

$$q = \left[\frac{2meE}{\hbar^2}\right]^{1/3}. \qquad (7)$$

We will make use of an average momentum squared in the state (6), $\langle p_z^2 \rangle = 0.78(\hbar q)^2$, and the average position $\langle z \rangle = 1.56/q$ to estimate the thickness of the 2DEG. The structural inversion asymmetry in V_z leads to the Rashba spin–orbit coupling (see equation (4)) and the Rashba coefficient α can be written as [39]

$$\alpha = \frac{\gamma_R e\langle E\rangle}{\hbar}, \qquad \gamma_R = \frac{\hbar^2\Delta\left(2E_g + \Delta\right)}{2mE_g\left(E_g + \Delta\right)\left(3E_g + 2\Delta\right)}, \qquad (8)$$

where Δ stands for the spin–orbit splitting in the valence band and E_g is the band gap. For InAs material, we adopt the value $\gamma_R = 110\,\text{Å}^2$.

Since, $[p_x, H_{xy}] = 0$, we consider p_x is the good quantum number and the eigenvalue of p_x can be written as [30, 31, 35]

$$p_x = \frac{m}{\hbar}\frac{d\varepsilon_\nu(k)}{dk} = \frac{ml}{2\hbar}\Delta_1\sin kl. \qquad (9)$$

The Hamiltonians (2) and (4) can be written in terms of annihilation and creation operators as

$$H_{xy} = \left(a^\dagger a + \tfrac{1}{2}\right)\hbar\omega_0 + \varepsilon_\nu(k), \qquad (10)$$

$$H_R = -\frac{\alpha ml}{2\hbar^2}\Delta_1\sin kl\,\sigma_y + \frac{i\alpha}{\ell_0\sqrt{2}}\left(a^\dagger - a\right)\sigma_x, \qquad (11)$$

To find the energy spectrum of the above Hamiltonian, it is convenient to rotate the Hamiltonian $\tilde{H}_{xyR} = \exp\left(-i\pi\sigma_x/4\right)(H_{xy} + H_R)\exp\left(i\pi\sigma_x/4\right)$ so that the eigenvalue

of p_x couples to σ_z. The new Hamiltonian can be written as $\tilde{H}_{xyR} = H_0 + H_1$, where H_0 is the diagonal part and H_1 is the non-diagonal part [4]:

$$H_0 = \left(a^\dagger a + \frac{1}{2}\right)\hbar\omega_0 - \frac{\Delta_1}{2}\frac{l}{\xi}\sin kl\, \sigma_z + \varepsilon_\nu(k), \quad (12)$$

$$H_1 = \frac{i\alpha}{\ell_0\sqrt{8}}\left(a^\dagger - a\right)\sigma_+ + \text{H.c.}, \quad (13)$$

where $\xi = \hbar^2/(\alpha m)$ is the spin-precession length, $\sigma_\pm = \sigma_x \pm i\sigma_y$ and H.c. stands the Hermitian conjugate. From equation (13), it is clear that the non-diagonal part couples the state differed by one quantum number. In a case, where $H_0 \gg H_1$, we use non-diagonal Hamiltonian H_1 as a perturbation. Based on the second-order perturbation theory, the energy spectrum of the nanowire can be written as

$$\varepsilon_{n,+1/2} = \left(n + \frac{1}{2}\right)\hbar\omega_0 - \frac{\Delta_1}{2}\frac{l}{\xi}\sin kl + \varepsilon_\nu(k)$$
$$+ \frac{\alpha^2\xi}{8\ell_0^2}\left[\frac{n}{\hbar\omega_0\xi - \Delta_1 l\sin kl} - \frac{n+1}{\hbar\omega_0\xi + \Delta_1 l\sin kl}\right], \quad (14)$$

$$\varepsilon_{n,-1/2} = \left(n + \frac{1}{2}\right)\hbar\omega_0 + \frac{\Delta_1}{2}\frac{l}{\xi}\sin kl + \varepsilon_\nu(k)$$
$$+ \frac{\alpha^2\xi}{8\ell_0^2}\left[\frac{n}{\hbar\omega_0\xi + \Delta_1 l\sin kl} - \frac{n+1}{\hbar\omega_0\xi - \Delta_1 l\sin kl}\right]. \quad (15)$$

We now turn to the calculation of spin–flip transition rate in parabolic nanowire modulated by periodic potential.

2.1. Electromagnetic field mediated spin transition rate

We apply the formalism of time-dependent perturbation theory to the interactions of parabolic nanowire modulated by longitudinal periodic potential with the classical electromagnetic radiation field [22, 40]. The total Hamiltonian of the nanowire SLs with electromagnetic field radiation is given by [23, 41]

$$H = H_0 + H_1 + H_A, \quad (16)$$

$$H_A = -\frac{e}{m}\mathbf{A} \cdot \mathbf{p} - \frac{\alpha e}{\hbar}A_y\sigma_x. \quad (17)$$

Equation (17) is treated as an external perturbation dependent on the position $\mathbf{r}$ and time t. The vector potential $\mathbf{A}(\mathbf{r}, t)$ of the electromagnetic field radiation is written as

$$\mathbf{A}(\mathbf{r}, t) = \sqrt{\frac{\hbar}{2\epsilon_r\omega_q V}}\hat{e}_{q\lambda}b_{q,\lambda}e^{i(q\cdot r - \omega_q t)} + \text{H.c.}, \quad (18)$$

where $\omega_q = c|\mathbf{q}|$, $b_{q,\lambda}$ annihilate photons with wave vector q, c is the velocity of light, V is the volume of the nanowire and ϵ_r is the dielectric constant of the nanowire. The polarization $\hat{e}_{q\lambda}$ with $\lambda = 1, 2$ are chosen as two perpendicular-induced photon modes in the nanowire. The polarization directions of the induced photon are $\hat{e}_{q1} = (\sin\phi, -\cos\phi, 0)$ and $\hat{e}_{q2} = (\cos\theta\cos\phi, \cos\theta\sin\phi, -\sin\theta)$ because we express $\mathbf{q} = q(\sin\theta\cos\phi, \sin\theta\sin\phi, \cos\theta)$. The above polarization vectors holds the relation as $\hat{e}_{q1} = \hat{e}_{q2} \times \hat{q}$, $\hat{e}_{q2} = \hat{q} \times \hat{e}_{q1}$

and $\hat{q} = \hat{e}_{q1} \times \hat{e}_{q2}$. Based on the Fermi–Golden Rule, the electromagnetic field mediated spin transition rate (i.e. the transition probability per unit time) in the nanowire modulated by longitudinal periodic potential is given by [40]

$$\frac{1}{T_1} = \frac{V}{(2\pi)^2\hbar}$$
$$\times \int d^3q \sum_{\lambda=1,2} |M_{q,\lambda}|^2\delta\left(\hbar\omega_q - \varepsilon_{0,-1/2} + \varepsilon_{0,+1/2}\right), \quad (19)$$

where the matrix element $M_{q,\lambda} = \langle n, 1/2|H_A|n, -1/2\rangle$ is found perturbatively. The spin transition rate (i.e. $(n, -1/2) \rightarrow (n, +1/2)$) is given by

$$\frac{1}{T_1} = \frac{\alpha^2 e^2\Delta_1 l\sin kl}{4\pi\hbar^4\xi\epsilon_r\epsilon_0 c^3}\left[1 - \frac{\alpha^2\xi^2}{4\ell_o^2\left\{(\hbar\omega_0\xi)^2 - (\Delta_1 l\sin kl)^2\right\}}\right]. \quad (20)$$

2.2. Phonon mediated spin transition rate

We now turn to the calculation of the phonon mediated spin relaxation rate in parabolic nanowire SLs. Following [7], the interaction between electron and piezo-phonon can be written as [18, 42–44]

$$u_{ph}^{q\alpha}(\mathbf{r}, t) = \sqrt{\frac{\hbar}{2\rho V\omega_{q\alpha}}}e^{i(q\cdot r - \omega_{q\alpha}t)}eA_{q\alpha}b_{q\alpha}^\dagger + \text{H.c.} \quad (21)$$

Here, ρ is the crystal mass density, V is the volume of the nanowire SLs, $b_{q\alpha}^\dagger$ creates an acoustic phonon with wave vector $\mathbf{q}$ and polarization $\hat{e}_\alpha$, where $\alpha = l, t_1, t_2$ are chosen as one longitudinal and two transverse phonon modes. Also, $A_{q\alpha} = \hat{q}_i\hat{q}_k e\beta_{ijk}e_{q\alpha}^j$ is the amplitude of the electric field created by phonon strain, where $\hat{q} = \mathbf{q}/q$ and $e\beta_{ijk} = eh_{14}$ for $i \neq k, i \neq j, j \neq k$. The polarization directions of the induced phonon are $\hat{e}_l = (\sin\theta\cos\phi, \sin\theta\sin\phi, \cos\theta)$, $\hat{e}_{t_1} = (\sin\phi, -\cos\phi, 0)$ and $\hat{e}_{t_2} = (\cos\theta\cos\phi, \cos\theta\sin\phi, -\sin\theta)$. Based on the Fermi Golden rule, the phonon-induced spin transition rate in the nanowire SLs is given by [38, 42]

$$\frac{1}{T_1} = \frac{(eh_{14})^2\alpha^2(\Delta_1 l\sin kl)^5}{70\pi\hbar^4\rho\xi\left[(\hbar\omega_0\xi)^2 - (\Delta_1 l\sin kl)^2\right]^2}\left(\frac{1}{s_l^5} + \frac{4}{3s_t^5}\right)$$
$$\times \left[1 - \frac{\alpha^2\xi^2}{4\ell_o^2\left\{(\hbar\omega_0\xi)^2 - (\Delta_1 l\sin kl)^2\right\}}\right]^3. \quad (22)$$

2.3. Spin-flip transition probability: Feynman disentangling technique

We used the Feynman disentangling technique [2, 28, 29] to find the transition probability of electron spins of the Hamiltonian associated with the Rashba spin–orbit coupling. Under the DP mechanism [25, 26], we consider the momentum $\mathbf{p}(t) = m\dot{\mathbf{r}}$ as a classical variable whose dependence on time t is generated by a Markovian process [27]. In this case, the Rashba spin–orbit Hamiltonian $\tilde{H}_R = \exp(-i\pi\sigma_x/4)H_R\exp(i\pi\sigma_x/4)$ can be written as

$$\tilde{H}_R(t) = \frac{\xi_0}{\xi}\hbar\omega_0\cos\omega_0 t\,(s_+ + s_-) - \frac{l}{\xi}\Delta_1\sin kl\, s_z, \quad (23)$$
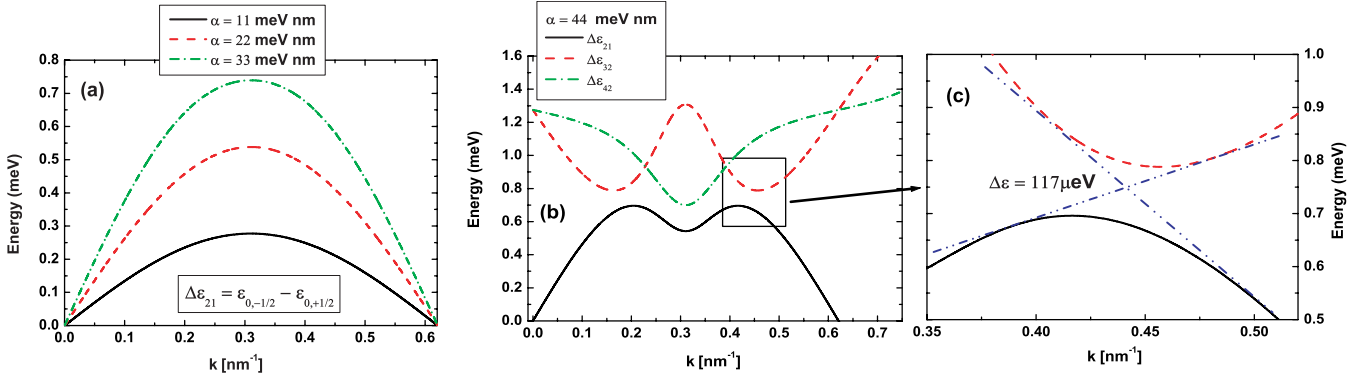
Figure 2. Dispersion relation: energy diff. versus k. (*a*) spin splitting energy increases and becomes maximum at $k = \pi/2l$. (*b*) It can be seen that the crossing between the states $|0, -1/2\rangle$ and $|1, +1/2\rangle$ takes place approximately at $k = 0.19\,\text{nm}^{-1}$ and $k = 0.43\,\text{nm}^{-1}$. Here we find the anticrossing width is approximately $117\,\mu\text{eV}$. We chose the material constants for InAs material as $m = 0.0239$, $\hbar\omega_0 = 1.3\,\text{meV}$, $\Delta_1 = 16\,\text{meV}$ and $l = 5.06\,\text{nm}$.

where $\xi = \hbar\omega_0\ell_0^2/\alpha$ is the spin-precession length, ξ_0 is the spin-orbital radius and $s_\pm = s_x \pm is_y$. The spin operators obey the $SU(2)$ algebra, $[s_+, s_-] = 2s_z$ and $[s_z, s_\pm] = \pm s_\pm$. The spin evolution operator, $U(0, t) = T\exp(-i/\hbar\int dt\,\tilde{H}_R(t))$ can be exactly found by utilizing Feynman disentangling method [2, 29] $U(0, t) = \exp(a(t)s_+)\exp(b(t)s_z)\exp(c(t)s_-)$, where $a(t)$, $b(t)$ and $c(t)$ are time-dependent functions that can be found exactly. In the disentangled form, the evolution operator can be written as

$$U(t) = e^{a(t)s_+}T\exp\left\{-\frac{i}{\hbar}\int_{t'=0}^{t}\left[\left(\frac{\xi_0}{\xi}\hbar\omega_0\cos\omega_0 t - \chi\right)s'_+\right.\right.$$
$$\left.\left. -\frac{l}{\xi}\Delta_1\sin kl\,s'_z + \frac{\xi_0}{\xi}\hbar\omega_0\cos\omega_0 t\,s'_-\right]dt'\right\}, \quad (24)$$

where T is the time ordering operator and

$$a(t) = -\frac{i}{\hbar}\int\chi(t')\,dt', \quad (25)$$

$$s'_\mu = \exp\left\{\frac{i}{\hbar}s_+\int\chi(t')\,dt'\right\}s_\mu\exp\left\{-\frac{i}{\hbar}s_+\int\chi(t')\,dt'\right\}. \quad (26)$$

By differentiating equation (26) with respect to 'a' and utilizing the initial condition $s'_\mu(0) = s_\mu$, we find the relations $s'_+ = s_+$, $s'_z = s_+a + s_z$, $s'_- = s_- - 2s_za - a^2s_+$. By substituting these relations in equation (24) and equating the coefficient of $s_+ = 0$, we find the differential equation in the form of

$$\frac{da}{dt} = -\frac{i}{\hbar}\left\{i\frac{\xi_0}{\xi}\hbar\omega_0\cos\omega_0 t\,(1 - a^2) - a\frac{l}{\xi}\Delta_1\sin kl\right\}. \quad (27)$$

In an analogous way, we can disentangle s_0 and s_- by differentiating equation (26) with respect to 'b' and 'c', respectively. However, a single function $a(t)$ needed to find the transition probability [29]. The differential equation (27) can be solved exactly for the case $k = 0$. Thus, its solution can be written as

$$a(t) = \frac{\exp\{-2i\xi_0\sin(\omega_0 t)/\xi\} - 1}{\exp\{-2i\xi_0\sin(\omega_0 t)/\xi\} + 1}. \quad (28)$$

The transition probability between the opposite spin states can be written as

$$\omega_{+1/2,-1/2} = \frac{|a|^2}{1 + |a|^2} = \sin^2\left(\frac{\xi_0}{\xi}\sin\omega_0 t\right). \quad (29)$$

From equation (29), it is clear that the spin–flip transition probability is enhanced with the Rashba spin–orbit coupling. At large value of Rashba spin–orbit coupling constant, the splitting of the peak value in the transition probability can be achieved due to the fact that the periodicity of the propagating waves in the crystal lattice changes with α. For the general case $k \neq 0$, we solve numerically the Riccati equation (27) to find the transition probability. In the disentangling operator scheme, as mentioned before, we write the momentum ($p(t) = m\dot{r}$) as a classical variable under the DP mechanism [25, 26], whose dependence on time t is generated by a Markovian process [27]. Thus the Riccati equation (27) can be treated as a non-relativistic case. In such a situation, if a particle with a magnetic moment travels with a relativistic speed in an electromagnetic field whose orbital movement can be regarded as a classical then one might expect a change in the spin behaviour (or in the particle polarization vector) [45]. Thus, from equation (29), one might expect to flip the spin completely (resonance case) [46] if $\sin\varphi = (n+1/2)\pi\xi/\xi_0$ where $\varphi = \omega_0 t$ and $n = 0, 1, 2, 3\ldots$.

3. Results and discussions

In figure 2(*a*), we have plotted energy versus k of InAs parabolic nanowire SLs in the presence of the Rashba spin–orbit coupling. We find Kramer's type degeneracy point at $k = \pm n\pi/l$ with $n = 0, 1, 2\ldots$. For the arbitrary values of k, the degeneracy can be lifted and we find the spin splitting energy. The splitted energy difference increases with the Rashba spin–orbit coupling strength and becomes maximum at $k = \pi/2l$. Note that this maxima point is also maxima of p_x (see equation (9)). In figure 2(*b*), we investigate the level crossing point associated with the spin states $|n, -1/2\rangle$ and $|n + 1, 1/2\rangle$. The crossing takes place at $k \approx 0.19\,\text{nm}^{-1}$ and $k \approx 0.43\,\text{nm}^{-1}$. Here the width of the anticrossing is approximately estimated as $117\,\mu\text{eV}$.

We now turn to the key results of the paper: the spin transition rate via electromagnetic field radiation, phonons and the DP mechanism [18, 24–26].

In figure 3, we plot the spin transition rate versus k between the spin states $|0, -1/2\rangle$ and $|0, +1/2\rangle$ under the
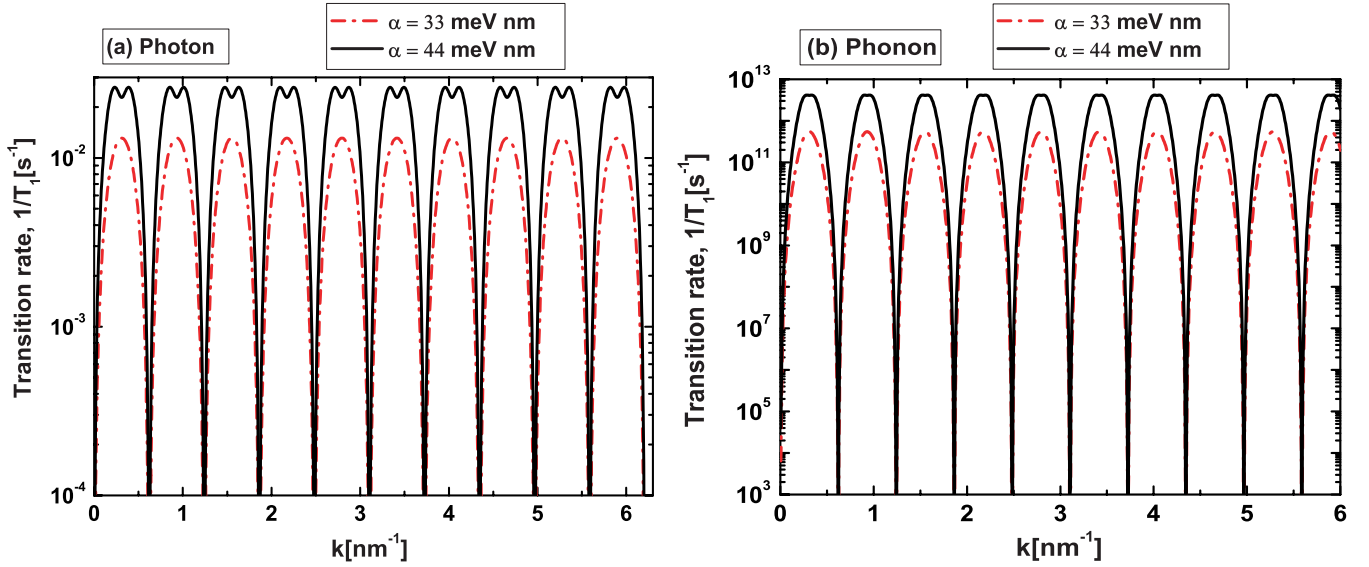
Figure 3. (*a*) Electromagnetic field mediated spin transition rate versus *k* in InAs nanowire SLs. In fact, the transition rate depends on the amplitude of the external field, if it is classical. However, since it is taken quantized in equation (18), the field amplitude does not influence figure 2(*a*). (*b*) Phonon mediated spin transition rate versus *k*. The dips in the transition rate (see solid lines) can be seen due to level crossing. Here we chose $\hbar\omega_0 = 1.3$ meV, $eh_{14} = 0.54 \times 10^{-5}$ erg cm^{-1}, $s_l = 4.2 \times 10^5$ cm s^{-1}, $s_t = 2.35 \times 10^5$ cm s^{-1}, $\rho = 5.6670$ g cm^{-3}, $\epsilon_r = 14.6$, $\Delta_1 = 16$ meV and $l = 5.06$ nm.
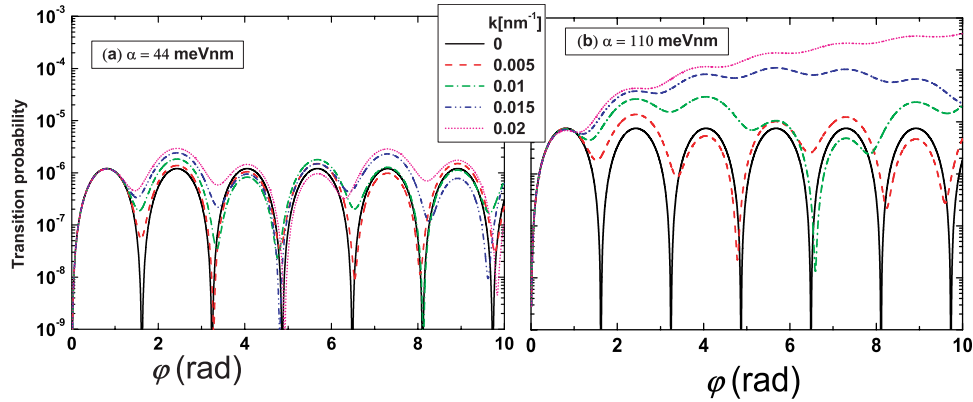

Figure 4. Transition probability, $w_{1/2,-1/2}$ versus φ in the InAs nanowire SLs. Here we chose $\Delta_1 = 72$ meV, $l = 53$ nm, $\hbar\omega_0 = 1.3$ meV, $\xi_0 = 1.5a_0$ and $a_0 = 0.053$ nm is the atomic Bohr radius.

influence of electromagnetic field radiation and phonons. It can be seen that the phonon mediated spin transition rate is several order of magnitude larger than the value mediated by electromagnetic field radiation because the electromagnetic field mediated transition rate vanishes like $\sin kl$ whereas, the phonon mediated spin transition rate vanishes like $(\sin kl)$ [5] (see equations (20) and (22)). The dips in the spin transition rate (see figure 2, solid lines) can be seen due to level crossing. The dips in the spin transition rate can be tuned with the application of the Rashba spin–orbit coupling. The cusp-like structure in the spin–flip rate was reported by the authors in [47, 48] for quantum dots system. For the case of parabolic nanowires modulated by longitudinal periodic potential, the dips found in the spin transition rate is new.

Finally, in figure 4, we plotted the transition probability versus time. In figures 4(*a*) and (*b*), we show that at $k = 0$ (see solid lines), the spin transition probability can be tuned with fixed time interval in the form of resonance. From

equation (29), we can write the theoretical condition for finding zero transition probability for the case ($k = 0$, solid lines (black) in figure 4) as

$$\sin\varphi = n\pi\frac{\xi}{\xi_0}, \qquad (30)$$

where $n = 0, 1, 2, 3 \ldots$. Condition (30) is satisfied by solid lines (black) in figure 4 and thus we find the zero transition probability at fixed interval of φ. Also, it can be seen that the spin–flip transition probability can be enhanced with the Rashba spin–orbit coupling. Next, we study the influence of the inclusion of the wavenumber (k). We find that there is a superposition effect between p_x and p_y in the evolution of the spin dynamics (see equations (24) and (27)) which induces the damping effect or spin echo in the transition probability with respect to time. For simplicity in equation (27), we consider

$$\sin k\ell = \frac{\xi_0\hbar\omega_0}{\Delta_1\ell}\cos\varphi. \qquad (31)$$

Here $\cos\varphi$ oscillates between -1 to $+1$ and for fixed value of k, the above condition (31) is satisfied several times with the variation of φ. Thus, one can find the zero spin transition probability at $\varphi = n\pi$. Whenever condition (31) is violated (i.e. $\sin k\ell \neq \xi_0 \hbar\omega_0 \cos\varphi/(\Delta_1\ell)$), then we find a superposition or spin echo (see figure 4 for the case $k \neq 0$). At large value of the Rashba coefficient α, the third term of equation (27) dominates over the first and second term and we find the spin freezing in the transition probability (see dashed line in figure 4(*b*)). Recently, similar type of results have been shown in [33].

4. Conclusion

In figure 2, we have demonstrated that the level crossing in parabolic nanowire SLs can be achieved with the accessible values of the strength of the Rashba spin–orbit coupling. The crossing point can be tuned to the lower values of k and vice versa with the application of the Rashba spin–orbit coupling. In figure 3, we have shown that the phonon mediated spin transition rate is several orders of magnitude larger than the electromagnetic field mediated spin transition rate. The dips in the spin transition rate can be found due to level crossing. Based on the Feynman disentangling technique method, in figure 4, we have shown that the transition probability can be tuned in the form of resonance at $k = 0$. For the arbitrary values of k, we have shown that there is a superposition effect which induces the damping in the transition probability. At sufficiently large values of the Rashba spin–orbit coupling coefficients, the spin transition probability freezes for the arbitrary values of k. It means that one cannot find the spin–flip transition rate at large value of k. In other words, manipulation (injection and detection) of spin qubits far away from the gamma point in quantum wires is not the ideal candidate for the purpose of building a solid state quantum computer. It might be possible that our theoretically investigated spin–flip transition rate in the NWSLs can be experimentally measured with current state-of-the art technology (see [9] for experimental set up).

Acknowledgments

References

[1] Prabhakar S and Raynolds J E 2009 *Phys. Rev. B* **79** 195307
[2] Prabhakar S, Raynolds J, Inomata A and Melnik R 2010 *Phys. Rev. B* **82** 195306
[3] Erlingsson S I, Egues J C and Loss D 2010 *Phys. Rev. B* **82** 155456
[4] Thorgilsson G, Egues J C, Loss D and Erlingsson S I 2012 *Phys. Rev. B* **85** 045306
[5] Nefyodov Y A, Shchepetilnikov A V, Kukushkin I V, Dietsche W and Schmult S 2011 *Phys. Rev. B* **83** 041307
[6] Prabhakar S, Raynolds J E and Melnik R 2011 *Phys. Rev. B* **84** 155208
[7] Prabhakar S, Melnik R V N and Bonilla L L 2012 *Appl. Phys. Lett.* **100** 023108
[8] Glazov M, Sherman E and Dugaev V 2010 *Physica E: Low dimensional Systems and Nanostructures* **42** 2157
[9] Liang D and Gao X P 2012 *Nano Lett.* **12** 3263
[10] Takahashi S, Deacon R S, Yoshida K, Oiwa A, Shibata K, Hirakawa K, Tokura Y and Tarucha S 2010 *Phys. Rev. Lett.* **104** 246801
[11] Bychkov Y A and Rashba E I 1984 *J. Phys. C: Solid State Phys.* **17** 6039
[12] Dresselhaus G 1955 *Phys. Rev.* **100** 580
[13] Trif M, Golovach V N and Loss D 2008 *Phys. Rev. B* **77** 045434
[14] Frantsuzov P, Kuno M, Janko B and Marcus R A 2008 *Nature Phys.* **4** 519
[15] Elzerman J M, Hanson R, Willems van Beveren L H, Witkamp B, Vandersypen L M K and Kouwenhoven L P 2004 *Nature* **430** 431
[16] Kroutvar M, Ducommun Y, Heiss D, Bichler M, Schuh D, Abstreiter G and Finley J J 2004 *Nature* **432** 81
[17] Golovach V N, Khaetskii A and Loss D 2004 *Phys. Rev. Lett.* **93** 016601
[18] Khaetskii A V and Nazarov Y V 2000 *Phys. Rev. B* **61** 12639
[19] Frey T, Leek P J, Beck M, Blais A, Ihn T, Ensslin K and Wallraff A 2012 *Phys. Rev. Lett.* **108** 046807
[20] Schomburg E *et al* 1998 *Phys. Rev. B* **58** 4035
[21] Voon L C L Y and Willatzen M 2003 *J. Appl. Phys.* **93** 9997
[22] Bastard G 1988 *Wave Mechanics Applied to Semiconductor Heterostructures* (New York: Wiley)
[23] Pietiläinen P and Chakraborty T 2006 *Phys. Rev. B* **73** 155315
[24] Dugaev V K, Sherman E Y, Ivanov V I and Barnaś J 2009 *Phys. Rev. B* **80** 081301
[25] Kiselev A and Kim K 2000 *Phys. Status Solidi* b **221** 491
[26] Pala M G, Governale M, Zülicke U and Iannaccone G 2005 *Phys. Rev. B* **71** 115306
[27] Schliemann J, Egues J C and Loss D 2003 *Phys. Rev. Lett.* **90** 146801
[28] Feynman R P 1951 *Phys. Rev.* **84** 108
[29] Popov V S 2007 *Phys.—Usp.* **50** 1217
[30] Kleinert P, Bryksin V V and Bleibaum O 2005 *Phys. Rev. B* **72** 195311
[31] Marinescu D C and Lung F 2010 *Phys. Rev. B* **82** 205322
[32] Lutchyn R M, Sau J D and Das Sarma S 2010 *Phys. Rev. Lett.* **105** 077001
[33] Echeverría-Arrondo C and Sherman E Y 2012 *Phys. Rev. B* **85** 085430
[34] Marinescu D C and Manolescu A 2012 *Phys. Rev. B* **85** 165302
[35] Bonilla L L, Álvaro M and Carretero M 2011 *Phys. Rev. B* **84** 155316
[36] Willatzen M, Melnik R, Galeriu C and Voon L L Y 2004 *Math. Comput. Simul.* **65** 385
[37] Stern F and Das Sarma S 1984 *Phys. Rev. B* **30** 840
[38] de Sousa R and Das Sarma S 2003 *Phys. Rev. B* **68** 155330
[39] de Andrada e Silva E A, La Rocca G C and Bassani F 1997 *Phys. Rev. B* **55** 16293
[40] Sakurai J J and Napolitano J 1994 *Modern Quantum Mechanics* (New York: Addison-Wesley)
[41] Avetisyan S, Pietiläinen P and Chakraborty T 2012 *Phys. Rev. B* **85** 153301
[42] Khaetskii A V and Nazarov Y V 2001 *Phys. Rev. B* **64** 125316
[43] Woods L M, Reinecke T L and Lyanda-Geller Y 2002 *Phys. Rev. B* **66** 161318
[44] Olendski O and Shahbazyan T V 2007 *Phys. Rev. B* **75** 041306
[45] Bargmann V, Michel L and Telegdi V L 1959 *Phys. Rev. Lett.* **2** 435
[46] Rabi I I 1937 *Phys. Rev.* **51** 652
[47] Bulaev D V and Loss D 2005 *Phys. Rev. Lett.* **95** 076805
[48] Bulaev D V and Loss D 2005 *Phys. Rev. B* **71** 205324